ACS APPLIED MATERIALS & INTERFACES

Letter

www.acsami.org

Aqueous Synthesis of Multidentate-Polymer-Capping Ag_2Se Quantum Dots with Bright Photoluminescence Tunable in a Second Near-Infrared Biological Window

Lianjiang Tan,[†] Ajun Wan,*[,‡] Tingting Zhao,[†] Ran Huang,[†] and Huili Li[§]

[†]School of Chemistry and Chemical Engineering and [§]School of Pharmacy, Shanghai Jiao Tong University, Shanghai 200240, China

[‡]State Key Laboratory of Pollution Control and Resources Reuse, National Engineering Research Center of Facilities Agriculture, Tongji University, Shanghai 200092, China

Supporting Information

ABSTRACT: A new strategy for fabricating water-dispersible Ag_2Se quantum dots (QDs) is presented. A multidentate polymer (MDP) was synthesized and used as a capping agent for Ag_2Se QDs. The MDP-capping Ag_2Se QDs were synthesized in aqueous solution at room temperature, which are highly photoluminescent in a second near-infrared (NIR-II) biological window and possess good photostability. These readily prepared NIR-II fluorescent nanoprobes have great potential for biomedical applications, especially useful for in vivo imaging.

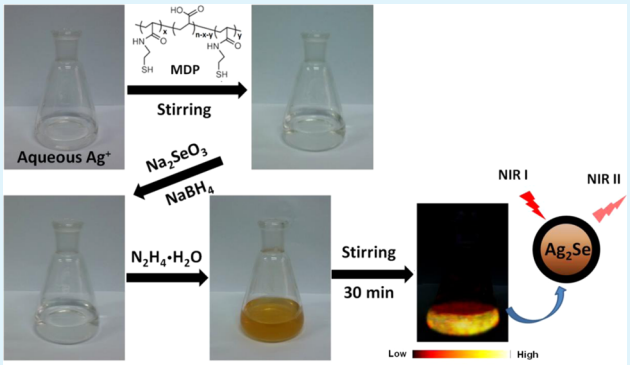

KEYWORDS: *Ag_2Se quantum dots, multidentate polymer, aqueous synthesis, second near-infrared*

1. INTRODUCTION

As an emerging class of fluorescent probes, second near-infrared (NIR-II) quantum dots (QDs) are currently under intensive study. Recent publications disclose that photoluminescence (PL) bioimaging in the NIR-II window (950−1400 nm) is appealing because of negligible albedo and autofluorescence, maximum penetration depth for deep tissue imaging, and high feature fidelity.[1−4] Compared with PL imaging of small animals in the visible region (400−750 nm) and first near-infrared region (NIR-I, 750−950 nm), NIR-II PL imaging is biologically preferred for its significantly improved signal-to-noise ratio. Great efforts have been devoted to developing NIR-II-emitting nanomaterials, such as PbS, PbSe, PbTe, CdHgTe QDs, etc.[5−8] These lead-, cadmium-, or mercury-containing QDs, however, are intrinsically toxic, which restrains their use for biological applications. Nanoscaled silver chalcogenides with minimal toxicity and narrow band gaps are promising candidates for NIR-II QDs.[9−12] Silver selenide (Ag_2Se) QDs with tunable emission in the NIR-II window have been successfully synthesized.[13] With an optimized emission centered at 1200−1300 nm, Ag_2Se QDs may be useful for in vivo imaging. However, few examples of facile and efficient synthesis of Ag_2Se QDs with bright NIR-II emission were reported. Yarema and co-workers prepared Ag_2Se QDs emitting in the NIR-II window in an organic phase with a low photoluminescence quantum yield (PLQY) of 1.7%.[13] Pang's group synthesized Ag_2Se QDs with PL emission in the wavelength range from 1080 to 1330 nm in an organic medium, using 1-octanethiol as the ligand.[14] The Ag_2Se QDs exhibited a maximum PLQY of 9.58%, which dramatically decreased to 3.33% when they were transferred to an aqueous phase via ligand exchange. More recently, Dong et al. obtained water-soluble NIR-II Ag_2Se QDs emitting at 1300 nm by a solvothermal method and subsequent surface modification.[15] The C18−PMH−PEG-capping QDs had an extraordinarily high PLQY of 29.4%. Nevertheless, hydrophobic QDs had to be synthesized in an organic phase at elevated temperature first and then transferred into water via ligand exchange to produce water-dispersible QDs.[16,17] Although QDs synthesized in an organic phase possess high PLQYs and photostability, the ligand-exchange process often requires strict conditions and is prone to deteriorate the optical properties of the QDs. In contrast, aqueous synthesis is straightforward, and the resultant QDs can be directly applied to biosystems, yet the relatively low PLQYs limit their biological applications. It is urgent to develop a simple and energy-saving technique for fabricating bright NIR-II Ag_2Se QDs.

Received: March 14, 2014
Accepted: April 29, 2014
Published: April 29, 2014

   dx.doi.org/10.1021/am5015088 | *ACS Appl. Mater. Interfaces* 2014, 6, 6217−6222

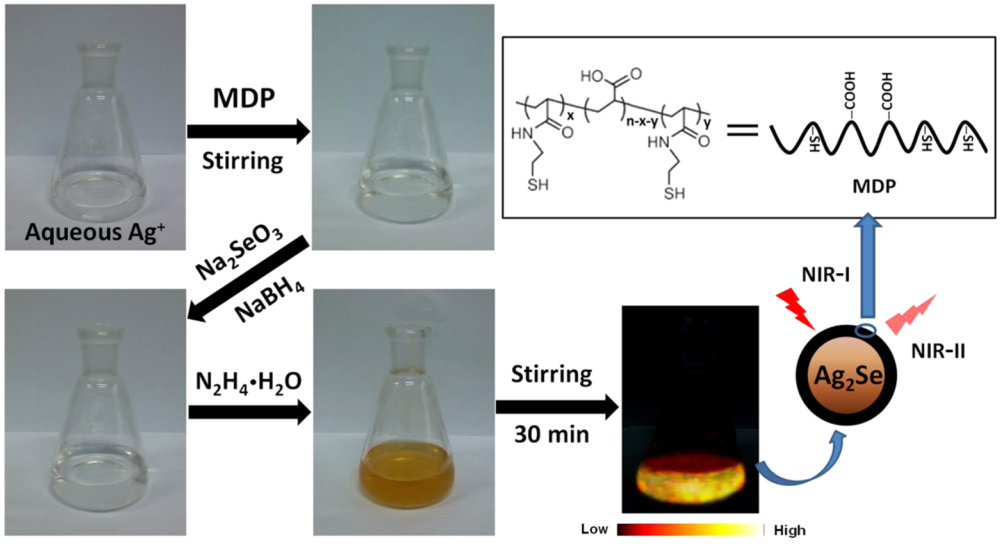

Figure 1. Photographic and schematic illustration of the synthetic procedure of MDP-capping Ag_2Se QDs.

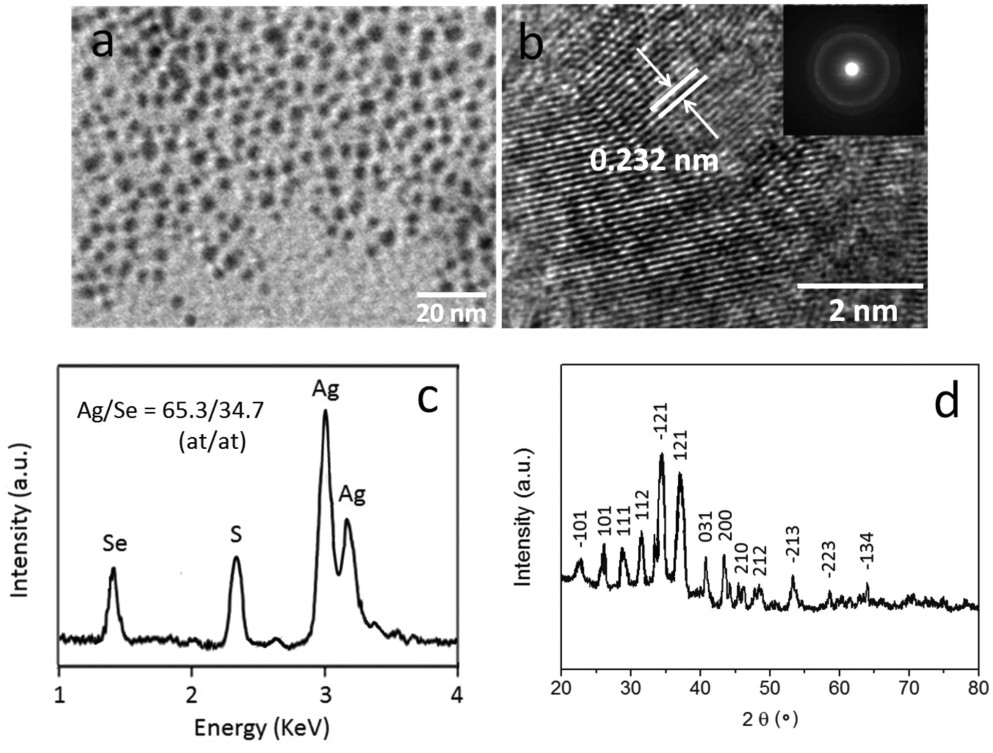

Figure 2. (a) TEM and (b) high-resolution TEM micrographs of MDP-capping Ag_2Se QDs. Inset: SAED pattern of the Ag_2Se QDs. (c) EDX spectrum and (d) XRD pattern of the Ag_2Se QDs. The reaction time for the QDs was 3 h.

2. RESULTS AND DISCUSSION

Chalcogen source and protecting ligands play key roles in the synthesis of silver chalcogenide QDs. It has been proven that QDs covered by monothiol ligands tend to aggregate over time because of the lability of the thiol−QD bonds.[18] Substitution of monothiol ligands by multidentate thiolated ligands is expected to improve the long-term stability of the QDs because multithiols in individual ligands afford a multidentate chelating effect and hence have stronger bonding affinity for the QDs. Hydrazine hydrate ($N_2H_4·H_2O$) has been reported as a good reducing agent for chalcogens, which can react with the hydrazine hydrate instantaneously to form an air-stable complex that can be directly used to synthesize metal−chalcogen nanocrystals under open conditions.[19] This complex chalcogen source favors PL enhancement of the resultant QDs owing to the protective effect of the hydrazine hydrate on the QDs.

Herein we describe a facile strategy for synthesizing highly photoluminescent Ag_2Se QDs in an aqueous phase at room temperature. A type of multidentate polymer (MDP), poly(acrylic acid)-*graft*-mercaptoethylamine (PAA-*g*-MEA), was utilized as the capping reagent. The use of MDP was not only for minimizing the hydrodynamic dimensions of QDs but also for improving their colloidal stability, photostability, and PLQY.[20] As depicted in Figure 1, MDP-capping Ag_2Se QDs

were prepared by the direct addition of the precursors in turn. The presynthesized MDP was added into an aqueous solution of $AgNO_3$ under stirring, followed by the addition of Na_2SeO_3 and $NaBH_4$ in sequence. Then $N_2H_4{\cdot}H_2O$ was injected into the solution, and the resultant mixture was stirred to produce Ag_2Se QDs stabilized by the MDP.

Specifically, 0.1 mL of 50 mmol/L $AgNO_3$ was placed in a conical flask, where 10 mmol of as-synthesized MDP was then added under stirring. Subsequently, 0.3 mL of 2 mmol/L Na_2SeO_3, 0.36 mg of $NaBH_4$, and 15.5 mL of $N_2H_4{\cdot}H_2O$ were added in turn. The resultant mixture was stirred at room temperature to allow the growth of QDs. After 0.5 h, the QDs with NIR-II emission were obtained. By adjustment of the reaction time, a series of MDP-capping Ag_2Se QDs with varied size and maximum PL emission were synthesized. The precipitates of QDs were collected by adding acetone and centrifugation, washed with ethanol, and redispersed in water.

The Fourier transform infrared spectrum (FTIR) of MDP-capping Ag_2Se QDs confirms that MDP exists on the QD surface as the ligand (Figure 1S in the Supporting Information, SI). The morphology of MDP-capping Ag_2Se QDs was observed by transmission electron microscopy (TEM; Figures 2a and 2Sa–c in the SI). The average size of the Ag_2Se QDs synthesized for different reaction times was determined by measuring the diameter of 100 nanoparticles in the TEM images. With an increase of the reaction time, the nanocrystals grew to larger dimension (Table 1). The high-resolution TEM

Table 1. Characteristics of the MDP-Capping Ag_2Se QDs Synthesized over Different Reaction Times

sample	reaction time (h)	emission (nm)	fwhm[a] (nm)	size TEM/ DLS (nm)	PLQY[b] (%)
S1	0.5	966	49	3.4 ± 0.3/ 5.3 ± 0.5	11.6 ± 1.2
S2	1	1021	54	4.0 ± 0.4/ 4.9 ± 0.5	11.8 ± 1.1
S3	1.5	1116	58	4.8 ± 0.5/ 6.9 ± 0.8	12.2 ± 1.4
S4	2	1190	59	5.5 ± 0.7/ 7.5 ± 1.0	11.1 ± 1.5
S5	3	1228	61	5.9 ± 0.8/ 8.1 ± 1.1	11.4 ± 1.0

[a]Full width at half-maximum. [b]Photoluminescence quantum yield.

micrograph (Figure 2b) shows lattice fringes of the Ag_2Se QDs with an interplanar spacing of 0.232 nm, which could be assigned to the (013) facets of an orthorhombic Ag_2Se (β-Ag_2Se) crystal.[21] The selected-area electron diffraction (SAED) image (Figure 2b, inset) displayed diffraction rings typical of β-Ag_2Se nanocrystals. The hydrodynamic dimension of the MDP-capping Ag_2Se QDs was measured by a dynamic light scattering (DLS) technique (Figure 2Sd–f in the SI). The size distribution histograms show that the average hydrodynamic dimension of the QDs increased with increasing reaction time (Table 1). Interestingly, in each case, the size obtained based on DLS was ca. 2 nm larger than that from the TEM observation, revealing the thickness of the MDP shell as ~2 nm. Energy-dispersive X-ray (EDX) analysis (Figure 2c) indicates the presence of elements silver, selenium, and sulfur in the MDP-capping Ag_2Se QDs, with an atomic ratio of silver to selenium close to the stoichiometry of bulk Ag_2Se. The element sulfur came from the thiols in the MDP. X-ray photoelectron spectrometry was employed to analyze the element valence state of the Ag_2Se QDs (Figure 3S in the SI). The two peaks at 373.82 and 367.59 eV are ascribed to the core levels of Ag $3d_{3/2}$ and Ag $3d_{5/2}$, respectively, suggesting that the oxidation state of silver was univalent in the QDs.[22] The peak at 54.06 eV is identified as Se 3d, indicative of the element selenium. Additionally, the X-ray diffraction (XRD) pattern (Figure 2d) verifies the QDs as β-Ag_2Se structure (JCPDS card no. 24-1041), in good accordance with the TEM observation and SAED results. Besides, the nanocrystal size of the QDs was calculated with the Scherrer equation based on the XRD pattern, which was 6.6 nm and close to the value determined by TEM.

The optical properties of the MDP-capping Ag_2Se QDs were investigated. Visible–NIR absorption and PL emission spectra of the QDs synthesized under varied conditions were recorded (Figure 3a,b). Both the absorption and emission spectra showed a red-shift behavior with extension of the reaction time. The maximum PL emission of all of the samples appeared in the NIR-II window. By alteration of the reaction time and thus tailoring of the QD size, the NIR-II emission of the QDs could be tuned from 966 to 1228 nm (Table 1). The full width at half-maximum increased slightly with prolonged reaction time (Table 1), most likely because of increasing size distribution during the growth of QDs. The PL excitation spectra of different QD samples (Figure 4S in the SI) indicate that PL of the QDs could be excited by light in the NIR-I region. This feature makes the use of QDs in in vivo imaging more convenient. The PLQY of all of the samples determined against a classic NIR fluorescent dye of indocyanine green (ICG) exceeded 11%, a fairly high value for a NIR-II fluorescent probe. It was found that the thickness of the MDP shell capping the QDs seemed not to be influenced by the reaction time. The compact polymer shell (~2 nm) results in a high degree of adsorption on the QD surface. By contrast, the coating thickness of various ligands (traditional bifunctional ligands and amphiphilic polymers) is often in the range of 4–60 nm.[23] The compact MDP shell helped to improve the PLQY of the Ag_2Se QDs up to 12.2%, high enough for deep tissue/organ in vivo imaging.

The transient PL data of the QDs fitted by a mono-exponential decay model show a characteristic lifetime of 135.3 ns (Figure 3c), close to previously reported values of Ag_2Se nanocrystal QDs.[13] The photostability of the MDP-capping Ag_2Se QDs was examined by exposing the QDs to continuous irradiation of a mercury lamp at ambient temperature (Figure 3d). The PL intensity changes of ICG are also shown for comparison. The QDs retained over 80% of the original PL intensity after 3 h of irradiation, whereas ICG was almost photobleached within the same period. In phosphate-buffered saline, fetal bovine serum, or mouse blood, the Ag_2Se QDs maintained high colloidal stability and exhibited no obvious decrease in the PL intensity after 7 days of storage at 37 °C (Figure 5S in the SI). These results indicate good chemical stability and photostability of the Ag_2Se QDs capped by the MDP, which are promising as a NIR-II probe for in vivo imaging.

We examined the cytotoxicity of the Ag_2Se QDs to two cell lines by trypan blue assay before the QDs were applied to small animal imaging. At a high QD concentration of 1.0 mg/mL, over 90% of the HeLa cells survived relative to the control group after incubation with the QDs for 24 and 48 h (Figure 6Sa in the SI). As for the L929 cells, the survival rate was 85.9%

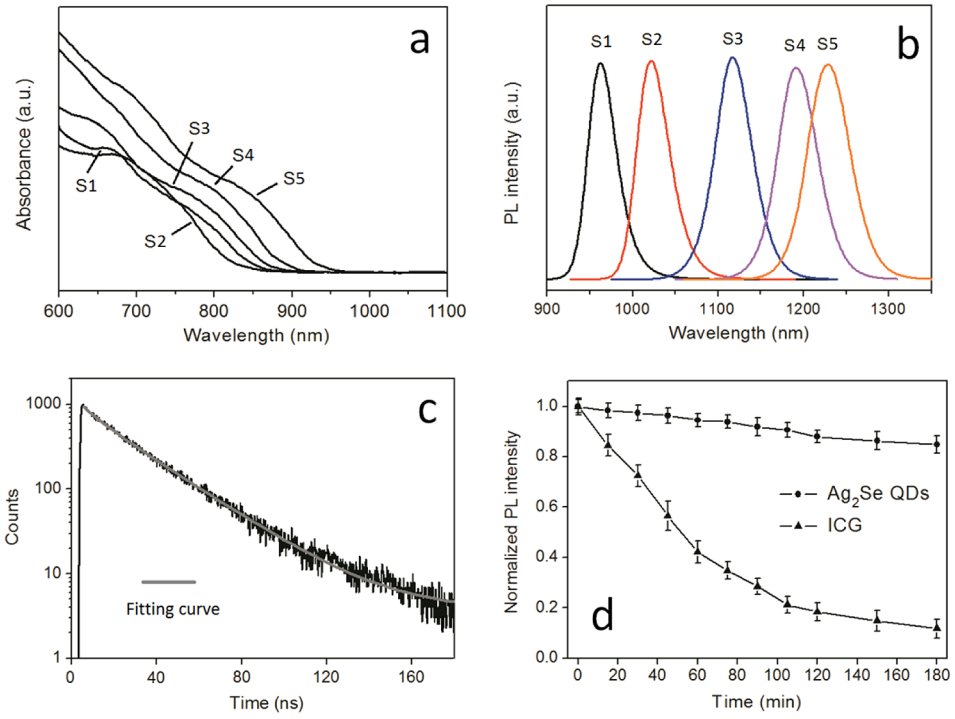

Figure 3. (a) Visible−NIR absorption and (b) emission spectra of MDP-capping Ag_2Se QDs synthesized with different reaction times (samples S1−S5 corresponding to 0.5, 1, 1.5, 2, and 3 h). The excitation was provided by a 488 nm laser. (c) PL lifetime measurements for the Ag_2Se QDs, exhibiting a decay time of 135.3 ± 11.5 ns according to monoexponential fitting. (d) PL intensity changes of the Ag_2Se QDs and ICG under continuous irradiation of a mercury lamp at a power output of 50 W for 3 h.

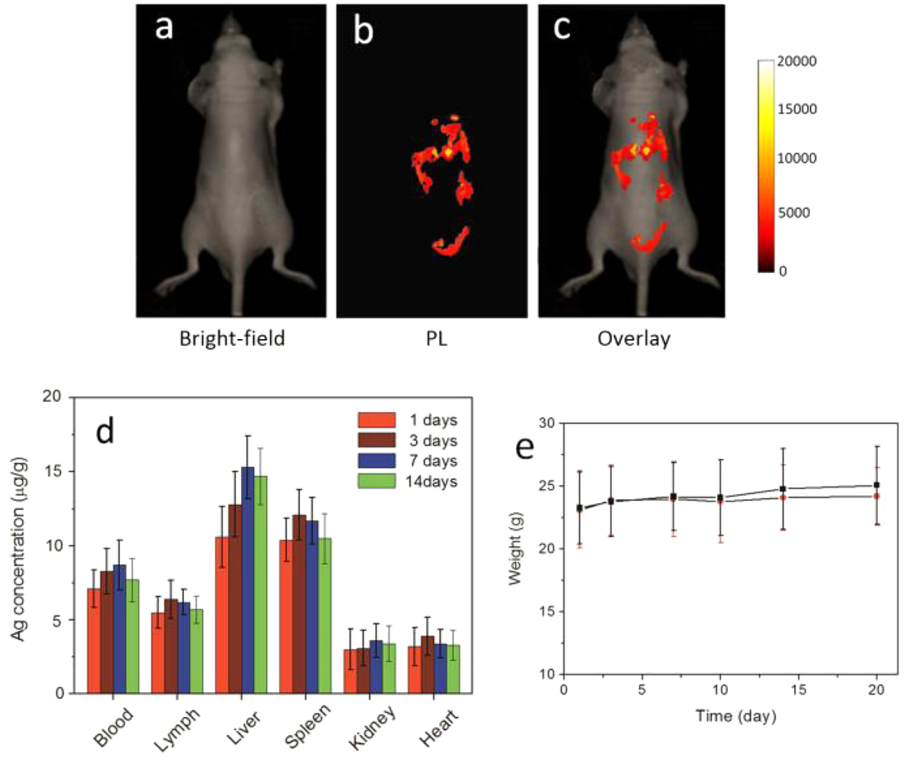

Figure 4. Bright-field images (a), in vivo fluorescence images (b), and overlay images (c) of a nude mouse at 12 h after tail vein injection of MDP-capping Ag_2Se QDs. (d) ICP-MS analysis of blood, lymph, and four major organs of the mice sacrificed at different time points after injection of MDP-capping Ag_2Se QDs. The error bars indicate plus and minus 1 standard deviation of the measurements for five treated mice. (e) Body mass of the mice treated with MDP-capping Ag_2Se QDs (red) and of untreated mice (black) over 20 days.

and 84.7% at 24 and 48 h, respectively (Figure 6Sb in the SI), suggesting ultralow toxicity of the MDP-capping Ag_2Se QDs.

In vivo imaging of nude mice was carried out to demonstrate potential therapeutic applications of the MDP-capping Ag_2Se

dx.doi.org/10.1021/am5015088 | ACS Appl. Mater. Interfaces 2014, 6, 6217−6222

QDs. A total of 10 μg of the QDs (reaction time = 1.5 h; 0.1 mg/mL in PBS) was administered into anesthetized nude mice by tail vein injection. After 12 h, one of the mice was imaged under irradiation of a 808 nm laser (Figure 4a–c). The signals received by an NIR-sensitive InGaAs camera were processed and coded and expressed by pseudocolor in an image. As can be clearly seen, the NIR-II PL signals derived from the QDs were visualized to be distributed in several regions of the mouse body via blood circulation. The readily detectable NIR-II signals and thus good contrast of the acquired images would facilitate diagnosis and treatment monitoring. Also, the emission from the QDs can be excited by NIR-I irradiation, which is able to penetrate deep into tissue and induce NIR-II PL efficiently.

The distribution of the nanoparticles in major organs as well as blood and lymph of the nude mice was evaluated over a period of 2 weeks, using inductively coupled plasma mass spectroscopy (ICP-MS; Figure 4d). Most of the Ag_2Se QDs were accumulated in the liver, spleen, and blood at 7 days postinjection. With prolonged time, the QDs were metabolized and the silver level in the mice body decreased. Besides, the weights of five nude mice injected with the QDs and five untreated mice were traced over a period of 20 days (Figure 4e). The two groups of mice showed similar weights in the data range without noticeable disparity. The treated mice did not exhibit other toxicity responses such as abnormal behavior either, which further confirmed the ultralow toxicity of the MDP-capping Ag_2Se QDs.

3. CONCLUSION

In summary, a facile procedure for the room temperature aqueous synthesis of Ag_2Se QDs with high PL efficiency in a NIR-II biological window was presented. Without nitrogen protection, pH adjustment, and energy enhancement, water-dispersible and photostable Ag_2Se QDs were synthesized simply through the stepwise addition of precursors. By adjustment of the reaction time of the precursors, Ag_2Se QDs with different emission wavelengths could be obtained. The capping reagent MDP played a pivotal role in the current synthesis because it acted as a layer of compact coating for the QDs. Another key was the reduced hydrazine hydrate, which afforded a protective surrounding to avoid oxidation of the QDs and thiols, reducing the surface defects of the QDs. Both of the factors result in relatively high PLQY. The results of this study would break previous limitations in synthetic conditions and provide a low-energy-consuming method for fabricating NIR-II QDs qualified for in vivo imaging.

■ ASSOCIATED CONTENT

Supporting Information

Relevant experimental procedure, results, and data not included in the manuscript. This material is available free of charge via the Internet at http://pubs.acs.org.

■ AUTHOR INFORMATION

Corresponding Author

*Tel/Fax: +86-21-34201245. E-mail: wanajun@sjtu.edu.cn.

Notes

The authors declare no competing financial interest.

■ ACKNOWLEDGMENTS

This work was financially supported by the Specialized Research Fund for the Doctoral Program of Higher Education (Grant 20130073120087), the National Natural Science Foundation (Grant 51173104), and the Nanometer Technology Program of Science and Technology Committee of Shanghai (Grant 11nm0503500).

■ REFERENCES

(1) Aswathy, R. G.; Yoshida, Y.; Maekawa, T.; Kumar, D. S. Near-Infrared Quantum Dots for Deep Tissue Imaging. *Anal. Bioanal. Chem.* **2010**, *397*, 1417–1435.

(2) Welsher, K.; Sherlock, S. P.; Dai, H. Deep-Tissue Anatomical Imaging of Mice Using Carbon Nanotube Fluorophores in the Second Near Infrared Window. *Proc. Natl. Acad. Sci. U.S.A.* **2011**, *108*, 8943–8948.

(3) Welsher, K.; Liu, Z.; Sherlock, S. P.; Robinson, J. T.; Chen, Z.; Daranciang, D.; Dai, H. A Route to Brightly Fluorescent Carbon Nanotubes for Near-Infrared Imaging in Mice. *Nat. Nanotechnol.* **2009**, *4*, 773–780.

(4) Smith, A. M.; Mancini, M. C.; Nie, S. M. Bioimaging: Second Window for in vivo Imaging. *Nat. Nanotechnol.* **2009**, *4*, 710–711.

(5) Bakueva, L.; Gorelikov, I.; Musikhin, S.; Zhao, X. S.; Sargent, E. H.; Kumacheva, E. PbS Quantum Dots with Stable Efficient Luminescence in the Near-IR Spectral Range. *Adv. Mater.* **2004**, *16*, 926–929.

(6) Wehrenberg, B. L.; Wang, C.; Guyot-Sionnest, P. Interband and Intraband Optical Studies of PbSe Colloidal Quantum Dots. *J. Phys. Chem. B* **2002**, *106*, 10634–10640.

(7) Murphy, J. E.; Beard, M. C.; Norman, A. G.; Ahrenkiel, S. P.; Johnson, J. C.; Yu, P. R.; Mićić, O. I.; Ellingson, R. J.; Nozik, A. J. PbTe Colloidal Nanocrystals: Synthesis, Characterization, and Multiple Exciton Generation. *J. Am. Chem. Soc.* **2006**, *128*, 3241–3247.

(8) Harrison, M. T.; Kershaw, S. V.; Burt, M. G.; Eychmuller, A.; Weller, H.; Rogach, A. L. Wet Chemical Synthesis and Spectroscopic Study of CdHgTe Nanocrystals with Strong Near-Infrared Luminescence. *Mater. Sci. Eng., B* **2000**, *69*, 355–360.

(9) Kershaw, S. V.; Susha, A. S.; Rogach, A. L. Narrow bandgap colloidal metal chalcogenide quantum dots: synthetic methods, heterostructures, assemblies, electronic and infrared optical properties. *Chem. Soc. Rev.* **2013**, *42*, 3033–3087.

(10) Sahu, A.; Qi, L.; Kang, M. S.; Deng, D.; Norris, D. J. Facile Synthesis of Silver Chalcogenide (Ag_2E; E = Se, S, Te) Semiconductor Nanocrystals. *J. Am. Chem. Soc.* **2011**, *133*, 6509–6512.

(11) Sahu, A.; Khare, A.; Deng, D. D.; Norris, D. J. Quantum Confinement in Silver Selenide Semiconductor Nanocrystals. *Chem. Commun.* **2012**, *48*, 5458–5460.

(12) Wang, D. S.; Zheng, W.; Hao, C. H.; Peng, Q.; Li, Y. D. A Synthetic Method for Transition-Metal Chalcogenide Nanocrystals. *Chem.—Eur. J.* **2009**, *15*, 1870–1875.

(13) Yarema, M.; Pichler, S.; Sytnyk, M.; Seyrkammer, R.; Lechner, R. T.; Fritz-Popovski, G.; Jarzab, D.; Szendrei, K.; Resel, R.; Korovyanko, O.; Loi, M. A.; Paris, O.; Hesser, G.; Heiss, W. Infrared emitting and photoconducting colloidal silver chalcogenide nanocrystal quantum dots from a silylamide-promoted synthesis. *ACS Nano* **2011**, *5*, 3758–3765.

(14) Zhu, C. N.; Jiang, P.; Zhang, Z. L.; Zhu, D. L.; Tian, Z. Q.; Pang, D. W. Ag_2Se Quantum Dots with Tunable Emission in the Second Near-Infrared Window. *ACS Appl. Mater. Interfaces* **2013**, *5*, 1186–1189.

(15) Dong, B.; Li, C.; Chen, G.; Zhang, Y.; Zhang, Y.; Deng, M.; Wang, Q. Facile Synthesis of Highly Photoluminescent Ag_2Se Quantum Dots as a New Fluorescent Probe in the Second Near-Infrared Window for in Vivo Imaging. *Chem. Mater.* **2013**, *25*, 2503–2509.

(16) Hong, G.; Robinson, J.; Zhang, Y.; Diao, S.; Antaris, A. L.; Wang, Q. In Vivo Fluorescence Imaging with Ag_2S Quantum Dots in

the Second Near-Infrared Region. *Angew. Chem., Int. Ed.* **2012**, *51*, 9818−9821.
(17) Zhang, Y.; Hong, G.; Zhang, Y.; Chen, G.; Li, F.; Dai, H.; Wang, Q. Ag_2S Quantum Dot: A Bright and Biocompatible Fluorescent Nanoprobe in the Second Near-Infrared Window. *ACS Nano* **2012**, *6*, 3695−3702.
(18) Liu, L.; Guo, X.; Li, Y.; Zhong, X. Bifunctional Multidentate Ligand Modified Highly Stable Water-Soluble Quantum Dots. *Inorg. Chem.* **2010**, *49*, 3768−3775.
(19) Kalasad, M. N.; Rabinal, M. K.; Mulimani, B. G. Ambient Synthesis and Characterization of High-Quality CdSe Quantum Dots by an Aqueous Route. *Langmuir* **2009**, *25*, 12729−12735.
(20) Kalasad, M. N.; Rabinall, M. K.; Mulimani, B. G. Facile Synthesis of Bioconjugated Fluorescent CdS Nanoparticles of Tunable Light Emission. *J. Phys. D: Appl. Phys.* **2010**, *4330*, 305301.
(21) Gu, Y. P.; Cui, R.; Zhang, Z. L.; Xie, Z. X.; Pang, D. W. Ultrasmall Near-Infrared Ag_2Se Quantum Dots with Tunable Fluorescence for In Vivo Imaging. *J. Am. Chem. Soc.* **2012**, *134*, 79−82.
(22) Xiang, J.; Cao, H.; Wu, Q.; Zhang, S.; Zhang, X.; Watt, A. A. R. L-Cysteine-Assisted Synthesis and Optical Properties of Ag_2S Nanospheres. *J. Phys. Chem. C* **2008**, *112*, 3580−3584.
(23) Pons, T.; Uyeda, H. T.; Medintz, I. L.; Mattoussi, H. Hydrodynamic Dimensions, Electrophoretic Mobility, and Stability of Hydrophilic Quantum Dots. *J. Phys. Chem. B* **2006**, *110*, 20308−20316.